

NUCLEAR MANY-BODY PHYSICS WHERE STRUCTURE AND REACTIONS MEET*

NAUREEN AHSAN AND ALEXANDER VOLYA

Department of Physics, Florida State University, Tallahassee, FL 32306, USA

The path from understanding a simple reaction problem of scattering or tunneling to contemplating the quantum nuclear many-body system, where structure and continuum of reaction-states meet, overlap and coexist, is a complex and nontrivial one. In this presentation we discuss some of the intriguing aspects of this route.

1. Introduction

Structure and reactions have traditionally been separate subjects of nuclear physics; however, recently the need for unification of our approach to open many-body systems has become apparent. The advances in experimental techniques led to observation of exotic nuclei which exist only due to complex interplay between many-body structural effects and reaction dynamics. Open mesoscopic systems like microwave cavities, quantum dots, nuclei, and even hadrons, play an increasingly important role in science and technology. A number of different theoretical techniques and approaches have been recently proposed on the path to a unified theory^{1,2,3}. In this presentation we discuss simple examples that stress the complexity of the structure-reaction borderline physics. We concentrate on the effects that the intrinsic structure of composite objects plays in quantum-mechanical scattering and tunneling processes. These processes are governed by non-perturbative physics with exponential sensitivity to various quantities. We examine two examples which, in our view, illuminate the physics of interest from two opposite sides. The first example is a model of the one-dimensional scattering of a two-body system from a potential, and the second case is a realistic example of ⁶He-neutron scattering. Despite complexity and non-perturbative nature we obtain an exact quantum-mechanical solution to

*The collaboration with V. Zelevinsky is highly appreciated. The work was supported by the U. S. Department of Energy, grant DE-FG02-92ER40750.

the model example, while in the realistic case the problem is solved with a Continuum Shell Model approach^{4,5} using an effective Hamiltonian. Both our examples highlight similar features related to the interplay of internal structure and reaction channels and emphasize the roles of symmetries and unitarity.

2. Reactions with a composite object: a model study

As our model example we consider a one-dimensional scattering problem where a projectile is a composite object made up of two particles bound by a potential $v(x_1 - x_2)$ which depends only on the relative distance between the particles. Here the particle coordinates are x_1 and x_2 , and the masses are m_1 and m_2 , respectively. This composite system interacts with an external scattering potential V . We assume that the external potential acts only on the second particle so that it depends only on the coordinate x_2 . Below we use the usual center-of-mass coordinate R and relative coordinate $r = x_1 - x_2$ and assume M and μ to be the total and reduced masses of the system, respectively. In these coordinates the total Hamiltonian is

$$H = -\frac{1}{2M} \frac{\partial^2}{\partial R^2} + h + V, \quad \text{where} \quad h = -\frac{1}{2\mu} \frac{\partial^2}{\partial r^2} + v(r)$$

is the intrinsic Hamiltonian of the system.

The channels $|n\rangle$ are the eigenstates of the intrinsic Hamiltonian: $h|n\rangle = \epsilon_n|n\rangle$, so that the asymptotic forms for the incoming-plus-reflected and transmitted waves are

$$|\Psi_-\rangle = e^{iK_0 R}|0\rangle + \sum_{n=0}^{\infty} C_{-,n} e^{-iK_n R}|n\rangle, \quad \text{and} \quad |\Psi_+\rangle = \sum_{n=0}^{\infty} C_{+,n} e^{iK_n R}|n\rangle. \quad (1)$$

Here $|\Psi_-\rangle$ includes the incoming wave in $n = 0$ channel, the ground state of the intrinsic potential; K_n is the channel momentum $K_n(E) = \sqrt{2M(E - \epsilon_n)}$ at a given total energy E . The sums in (1) implicitly contain both open and closed channels depending on whether the corresponding $K_n(E)$ is real or purely imaginary. In the expression we use the principal value of the square root so that the reflected waves in closed channels exponentially fall off. The conservation of the center-of-mass flux in the open channels leads to the unitarity relation

$$\sum_{n \text{ open}} (R_n + T_n) = 1, \quad \text{where} \quad R_n = \frac{K_n}{K_0} |C_{-,n}|^2 \quad \text{and} \quad T_n = \frac{K_n}{K_0} |C_{+,n}|^2 \quad (2)$$

are, respectively, the reflection and transmission probabilities in the n -th channel.

We model the external potential with a delta-peak, and only the second particle is assumed to interact with it: $V(x_2) = \alpha\delta(x_2)$. We implement a usual treatment of a delta-potential by separating left and right regions denoted by $-$ and $+$ subscripts, respectively. The principal complication in this problem comes from the boundary condition on x_2 being incompatible with the center-of-mass coordinates. The boundary conditions projected onto the m -th quantum state result in a system of linear equations:

$$\sum_n [C_{+,n} \langle m|D(k_n)|n\rangle - C_{-,n} \langle m|D(-k_n)|n\rangle] = \langle m|D(k_0)|0\rangle, \quad (3)$$

$$\sum_n [C_{+,n} \langle m|Q(k_n) - 2m_2\alpha D(k_n)|n\rangle - C_{-,n} \langle m|Q(-k_n)|n\rangle] = \langle m|Q(k_0)|0\rangle.$$

Here for simplicity of notations we use an intrinsic momentum shift operator $D(k) = e^{ikr}$ and the operator $Q(k) = i[\rho k D(k) - D(k)p]$ where $p = -i\partial/\partial r$ and $\rho = m_2/m_1$.

We show our results for a case where the binding potential is given by that of a harmonic oscillator. The expectation value of the momentum shift operator can be expressed analytically with the Associated Laguerre Polynomials. We choose ω as our energy scale leaving relative kinetic energy $\mathcal{E} = E/\omega - 1/2$ and relative energy scale of delta-peak $\Delta = M\alpha^2/\omega$ as energy parameters.

The problem expressed by equations (3) is that of an infinite set of linear equations which had to be solved by truncating the space and including only a finite number of intrinsic states. The momentum-shifts for highly virtual channels occur along the imaginary axis; therefore the momentum-shift operator matrix elements are exponentially divergent for these channels, and so are the corresponding coefficients $C_{\pm,n}$. This shows a mathematically complex behavior near the barrier where the boundary conditions are satisfied by cancellations of exponentially divergent terms. Physically, however, highly-virtual excitations decay fast leading to a regular behavior away from the delta peak. Thus, this well-formulated problem of quantum mechanics appears to be quite challenging mathematically. The proof of validity of the truncation mentioned above is an important issue addressed in Ref.⁶. The flux conservation (2) provides an additional test of consistency and convergence.

The transmission probabilities for the two lowest channels resulting from the scattering of an oscillator-bound system off a delta function are shown

in Fig.1. The figure demonstrates some of the generic features inherent to the composite-particle scattering. The incident wave contains a composite particle in the ground state and the number of open reflection/transmission channels depends on the incident kinetic energy. For harmonic oscillator the threshold energies for channel-opening correspond to integral values of \mathcal{E} . At low energies, $\mathcal{E} < 1$, transmission and reflection only in the ground state are possible, and $T_0 + R_0 = 1$. Once the $\mathcal{E} = 1$ threshold is crossed transmission and reflection in the first excited oscillator state are also possible and the total flux is then shared among all four processes: $T_0 + T_1 + R_0 + R_1 = 1$. The number of open channels increases with each integral value of \mathcal{E} . The redistribution of probabilities at the threshold values leads to cusps in the cross sections^{7,8}. A careful examination of Fig.1 reveals the appearance of such sharp points at thresholds. In addition to these, an interesting resonant-type behavior can be noted in the transmission (and reflection, not shown here) probabilities associated with peaks that do not coincide with threshold energies. This resonant behavior is related to the intrinsic structure. The case of a non-composite particle is a standard textbook example, where the reflection $R = (1 + 2[\mathcal{E}/\Delta])^{-1}$ depends only on kinetic energy relative to the delta strength. In the figure, this non-composite limit for the corresponding kinematic conditions is shown with a thick solid line that has no oscillations. Within our model this limit can be continuously reached when $\rho \rightarrow \infty$, namely, when the mass of a non-interacting particle approaches zero.

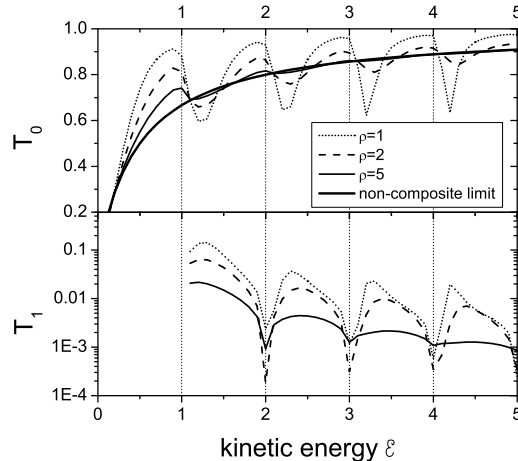


Figure 1. Transmission probabilities for the first two channels of a composite particle through the delta barrier as a function of kinetic energy \mathcal{E} at $\Delta = 1$ with different ρ 's.

For the mass ratio ρ of the orders of 1 or smaller the internal structure

plays an increasingly important role in the dynamics. The sensitivity of R and T to the parameters of the model becomes large and there appear resonances associated with the internal structure.

3. Interplay of structure and reactions in the unified continuum shell model approach

We study our second, realistic example of ${}^7\text{He}+n$ scattering using a Continuum Shell Model approach which is discussed in a series of recent publications^{9,4}. The projection formalism that lies in the foundation of the model dates back to Feshbach¹⁰. The detailed study can be found in the textbooks^{11,12}, and the previous development of the method was reviewed by Rotter¹³. This method is actively used in diverse areas of open quantum many-body systems from molecular and condensed matter physics¹⁴ to multi-quark systems¹⁵. We review some of the important ingredients below.

3.1. Structure

The part of the Hilbert space related to the particle(s) in the continuum is eliminated with the projection formalism. As a result the “intrinsic” dynamics is given by the effective Hamiltonian

$$\mathcal{H}(E) = H_0 + \Delta(E) - \frac{i}{2}W(E). \quad (4)$$

Here the full Hamiltonian H_0 is restricted to the intrinsic space, and is supplemented with the Hermitian term $\Delta(E)$ that describes virtual particle excitations into the excluded space. The imaginary term $iW(E)/2$ represents irreversible decays to the continuum. These new terms in the projected Hamiltonian (4) are given in terms of the matrix elements $A_1^c(E) = \langle 1|H_0|c; E\rangle$ of the full original Hamiltonian that link the internal states $|1\rangle$ with the energy-labeled external states $|c; E\rangle$ in the following manner:

$$\Delta_{12}(E) = \text{P.v.} \int dE' \sum_c \frac{A_1^c(E')A_2^{c*}(E')}{E - E'}, \quad W_{12}(E) = 2\pi \sum_{c(\text{open})} A_1^c A_2^{c*}. \quad (5)$$

The properties of the effective Hamiltonian (4) are as follows:

1. For unbound states, above the decay thresholds, the effective Hamiltonian is non-Hermitian which reflects the loss of probability from the intrinsic space.

2. The Hamiltonian has explicit energy dependence, making the internal dynamics highly non-linear.

3. The solution for each individual nucleus is coupled to all the daughter systems via a chain of reaction channels.

4. Even with two-body forces in the full space, the many-body interactions appear in the projected effective Hamiltonian.

5. The eigenvalue problem $\mathcal{H}(E)|\alpha\rangle = \mathcal{E}|\alpha\rangle$ represents a condition for the many-body resonant Siegert states, for which the regular wave function is matched with the purely outgoing one at infinity. Below all decay thresholds the imaginary part disappears and the problem is equivalent to that of a traditional shell model. Above decay thresholds, in general, there are no real energy solutions, i.e., the stationary state boundary condition cannot be satisfied. The complex energy eigenvalues correspond to poles of the scattering matrix.

3.2. Reactions and Unitarity

The picture where the nuclear system is probed from “outside” is given by the transition matrix defined within the general scattering theory¹¹,

$$T^{ab}(E) = \sum_{12} A_1^{a*}(E) \left(\frac{1}{E - \mathcal{H}(E)} \right)_{12} A_2^b(E). \quad (6)$$

The poles of this transition matrix and the related full scattering matrix $S = 1 - 2\pi iT$ are the eigenvalues of the effective Hamiltonian. The reaction theory is fully consistent with the structure description in Sec. 3.1. However, many-body complexity, numerous poles, overlapping resonances and energy dependence can make the observable cross-section quite different from a collection of individual resonance peaks.

The transition matrix (6) with the dimensionality equal to the number of open channels can be written as $T = \mathbf{A}^\dagger \mathcal{G} \mathbf{A}$, where the full effective Green's function $\mathcal{G}(E) = 1/(E - \mathcal{H})$ includes the loss of probability into all decay channels. The non-Hermitian part of Eq.(4) is factorized as $W = 2\pi \mathbf{A} \mathbf{A}^\dagger$, where \mathbf{A} represents a channel matrix (a set of column-vectors A_1^c for all the channels c). As shown in Refs.^{16,17}, iteration of the Dyson equation using the definitions $\mathcal{H} = H - iW/2$ and $G = (E - H)^{-1}$ leads to the following transition and scattering matrices

$$T = \frac{R}{1 + i\pi R}, \quad S = \frac{1 - i\pi R}{1 + i\pi R}. \quad (7)$$

The matrix $R = \mathbf{A}^\dagger \mathbf{G} \mathbf{A}$ is analogous to the R -matrix of the standard reaction theory; it is based on the Hermitian part of the Hamiltonian $H =$

$H_0 + \Delta$. Thus, the factorized nature of the intrinsic Hamiltonian and the appearance of the same effective operator in the scattering matrix are important consequences of unitarity.

3.3. The He example

In Fig.2 we consider a realistic example of ${}^6\text{He}$ -neutron scattering. The parameters of the model are given by the intrinsic shell model Hamiltonian from Ref. ⁵ within the p-shell valence space. The continuum reaction physics is modelled by the Woods-Saxon Hamiltonian. The model is discussed in-depth in Ref. ⁵, where the entire chain of He isotopes is solved in a coupled manner. For simplification of this discussion we consider states in ${}^6\text{He}$ to be bound, and concentrate on the role of the internal structure in scattering with a neutron. Energies are quoted here relative to the alpha particle ground state.

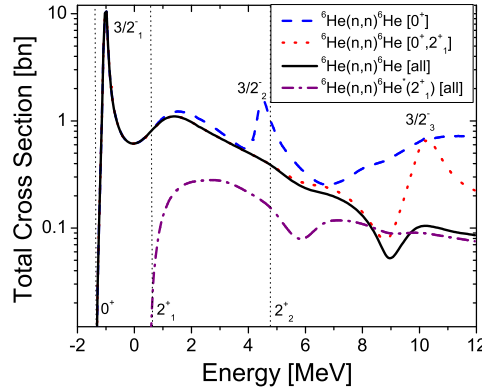


Figure 2. Cross-section for the neutron scattering of ${}^6\text{He}$ in 0^+ ground state. The solid curve is the total elastic cross-section, while the dashed and dotted curves correspond to the cases when only 0^+ channel (final state of ${}^6\text{He}$) and both 0^+ and 2_1^+ channels are included, respectively. The dash-dot curve shows inelastic cross-section with ${}^6\text{He}$ in the 2_1^+ final state. Thresholds for the lowest three channels, 0^+ , 2_1^+ and 2_2^+ , are marked with vertical grid lines. Locations for three $3/2^-$ resonances in ${}^7\text{He}$ are indicated.

1. At low energies the peak in the cross-section corresponds to a narrow resonance, $E_r = -1.02$ MeV, and a width of 91 keV which corresponds well to a spectroscopic factor $C^2S = 0.498$.

2. The threshold to a second decay-channel (decay to a 2^+ , 1.89 MeV excited state in ${}^6\text{He}$) is at 0.515 MeV. At this energy there is a cusp in the cross-section; however, for a p-wave neutron the curve is smooth unlike that for an s-wave.

3. The resonance corresponding to the second $3/2^-$ state (5.510 MeV excitation energy) in ${}^7\text{He}$ appears at 4.494 MeV only when all other decay channels are ignored (dashed line in Fig.2). This state has a large width

to decay into 2^+ final state in ${}^6\text{He}$, the $C^2S=1.03$ which makes resonance peak impossible to observe.

4. Conclusions

In this work we target the issue of internal degrees of freedom in scattering processes. We use two models, which are very different in their nature and nicely show different aspects of the physics of interest. The exactly solved simple one-dimensional scattering shows an unusual resonant behavior associated with the composite nature of the incident system. An application of the Continuum Shell Model was demonstrated and discussed within a realistic example. Interplay between channels, unitarity, and distribution of flux are common to both examples and lead to generic near-threshold behavior. We emphasize the importance of future theoretical developments toward a unified description of structure and reactions.

References

1. N. Michel et al., Phys. Rev. C **67** (2003) 054311; Phys. Rev. C **70** (2004) 064313.
2. K. Bennaceur et al., Nucl. Phys. A **671** (2000) 203.
3. D. Eppel and A. Lindner, Nucl. Phys. A **240** (1975) 437.
4. A. Volya and V. Zelevinsky, Phys. Rev. Lett. **94** (2005) 052501.
5. A. Volya and V. Zelevinsky, Phys. Rev. C **74** (2007) 064314.
6. N. Ahsan, Role of internal degrees freedom of a composite object in reactions, 2007, Prospectus for Ph.D., Department of Physics, Florida State University.
7. L. D. Landau and E. M. Lifshitz, Quantum mechanics. Non-relativistic theory. (Pergamon Press, New York, 1981).
8. A. I. Baz, I. B. Zeldovich and A. M. Perelomov, Scattering, reactions and decay in nonrelativistic quantum mechanics (Nauka, Moscow, 1971).
9. A. Volya and V. Zelevinsky, Phys. Rev. C **67** (2003) 054322.
10. H. Feshbach, Ann. Phys. **5** (1958) 357; Ann. Phys. **19** (1962) 287.
11. C. Mahaux and H. A. Weidenmüller, Shell-model approach to nuclear reactions (North-Holland Pub. Co., Amsterdam, London, 1969).
12. H. Feshbach, Theoretical nuclear physics : nuclear reactions (Wiley, New York, 1991).
13. I. Rotter, Rep. Prog. Phys. **54** (1991) 635.
14. A. Volya and V. Zelevinsky, J. Opt. B **5** (2003) S450.
15. N. Auerbach, V. Zelevinsky and A. Volya, Phys. Lett. B **590** (2004) 45.
16. L. Durand, Phys. Rev. D **14** (1976) 3174.
17. V. V. Sokolov and V. G. Zelevinsky, Nucl. Phys. A **504** (1989) 562.